

# **Design of an Output Mode Cleaner to Enable DC Readout in the LIGO 40-Meter Interferometer**

Mentor: Alan Weinstein, Co-mentor: Robert Ward

Author: Marcus Ng

# Design of an Output Mode Cleaner to Enable DC Readout in the LIGO 40-Meter Interferometer

Mentor: Alan Weinstein, Co-mentor: Robert Ward

## Introduction/Background

LIGO uses a Michelson interferometer (IFO) setup with Fabry-Perot Cavities in the arms to detect gravitational waves. As the test bed for Advanced LIGO, the LIGO 40m Lab incorporates and improves upon the different components of LIGO. A gravitational wave will stretch one interferometer arm, while at the same time it will compress the other arm. The stretching and squeezing occur alternatively with the direction of stretching orthogonal to the direction of squeezing. In initial LIGO, RF sidebands are placed on the beam before it enters the IFO. Then the light detected at the asymmetric port of the interferometer is beat against the RF. The beats contain information about the position of the mirrors, allowing detection of relative position of the mirrors, thus allowing detection of gravitational waves. This is known as RF readout. For AdLIGO, the RF sidebands will carry too much noise to use as a reference beam, so instead the carrier light will be used as a reference. Because the RF sidebands and all higher order light carry no gravitational wave information, they must be removed from the signal at this port. To do this, a special Fabry Perot Cavity, called an Output Mode Cleaner will be constructed at the asymmetric port of the interferometer.

In this paper we describe the design of an output mode cleaner (OMC) for the LIGO 40m IFO. A mode cleaner consists of a Fabry-Perot cavity that has the characteristic that it tightly controls the transverse profile of the beam such that the HOM have a large Guoy phase shift, so that they are filtered out. A mode cleaner will pass the  $TEM_{00}$  beam through the cavity with near unity transmission. Mode cleaners are often constructed in a triangular geometry so that the reflected beam that results from the higher transverse modes (i.e., the “junk light”) will not retroreflect to the interferometer. This “mode cleaning” will allow a much cleaner signal, reducing the noise produced, greatly improving the LIGO 40m performance as a whole. Additionally, the output mode cleaner will remove any RF sidebands. Removing the RF sidebands will allow DC detection with reduced noise from the RF sidebands.

## Objectives

The goal of this project is to design the top-level parameters for an Output Mode Cleaner for the LIGO 40m IFO. This will entail optimizing various mirror and cavity parameters such as the reflectivity of the coupling mirrors, the cavity aspect ratio, and the radius of curvature for the one curved mirror. The Output Mode cleaner should maximize the desired resonant  $TEM_{00}$  Gaussian profile beam, while at the same time effectively filter the higher order transverse excited modes, and also filtering off the RF sidebands.

Constructing an extremely high finesse cavity will ensure that even small frequency deviations from resonance will fall off in transmissivity very quickly. Additionally, it will be important to select an aspect ratio that minimizes the amount of counter-propagating modes (which would be injected back into the interferometer, and then be reflected back to the GW detection port, thereby producing noise).

## Design Criteria for the Output Mode Cleaner

- Filter  $TEM_{01}$  and all higher order TEMs
- Filter 33 and 166 MHz RF sidebands and HOM
- Stable cavity (negligible diffraction losses)
- Strong output  $TEM_{00}$  signal, better than 99.5% Transmission
- Angle of incidence must be great enough to prevent backreflection to the IFO
- Body material must have thermal expansion low enough that PZT only need compensate for length changes  $< 1 \mu\text{m}$
- Reduction in transmission of all other light to at most  $10^{-2}$ .
- Well-defined beam waist size and location, for mode-matching into the cavity
- Well defined (and suitably minimized) level of astigmatism
- External mode matching telescope to focus incident beam on beam waist and match astigmatism
- Internal angles must be great enough to avoid backreflection and counter-propagating light
- Reliable dither-locking

## Approach

In this paper, we describe the analysis and design of the output mode cleaner through modeling. Completed modeling and design:

- Model the transmission for TEM<sub>00</sub>
- Model the cavity reflection
- Model the cavity transmission for higher order TEMs and RF sidebands
- Model the astigmatism
- Determine ideal cavity length due to requirements on the g-factor for cavity stability
- Model g-factor at reasonable cavity length as a function of available Radius of Curvature (ROC)
- Predict the HOM coupling due to transverse displacement of the beam
- Predict the HOM coupling due to angular displacement of the beam
- Predict the HOM coupling due to cavity astigmatism relative to the astigmatism due to the incident beam
- Predict the HOM coupling due to mode mismatching with the incident beam
- Model the amount of counter-propagating light in the cavity

See Appendix B for a Final Summary of Work.

## What is a Mode Cleaner? Why use one?

A simple Fabry-Perot cavity is an optical cavity consisting of two or more mirrors. The mirrors are set up linearly such that the reflected light is retroreflected back, while the transmitted light is collinear with the incident beam (see Figure 1). When the laser light enters the cavity, the reflection is very high, except when the laser frequency is at resonance with the cavity, which occurs when the cavity length is some number of half integer wavelengths of the laser (see Appendix A: Resonance Condition and Peak Characteristics). A critically coupled Fabry-Perot cavity is a special case of Fabry-Perot cavity that allows near unity transmission for a particular longitudinal mode of the laser beam, and in general a Fabry-Perot cavity will resonantly enhance the phase shift of the light in the cavity. For an interferometer setup, the two arms will result in phase shifted reflected light. See Appendix A: The Physics behind a Fabry-Perot Cavity.

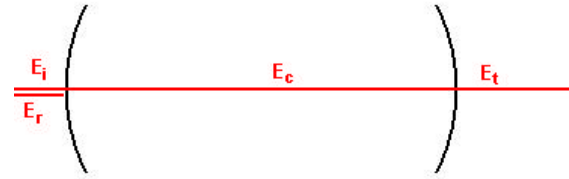


Figure 1. Simple Fabry-Perot Cavity

Resonant cavities have both longitudinal and transverse modes of excitation. The transverse modes of excitation can be expressed in a nearly complete basis as Hermite-Gaussian modes. For gravitational wave detection, the lowest order mode state produces the clearest, simplest results, while the higher order excited modes produce noise in the signal.

A mode cleaner is a specially designed Fabry-Perot optical cavity. It consists of two or more mirrors, where the cavity length and mirror specifications are selected such that the higher order TEMs and other “dirty” light do not resonate in the cavity. Generally for a cavity with more than two mirrors, the cavity geometry is selected so the reflected light is not collinear with the input beam.

Retroreflected light along the path of the laser is highly undesirable, as it would enter the IFO, which could then be reflected back to the GW detection port, producing noise. To minimize this, the angle between the incident and reflected beams should be fairly large. Selecting the aspect ratio of the MC determines the incident and reflected angles. See Figure 2 for MC geometries.

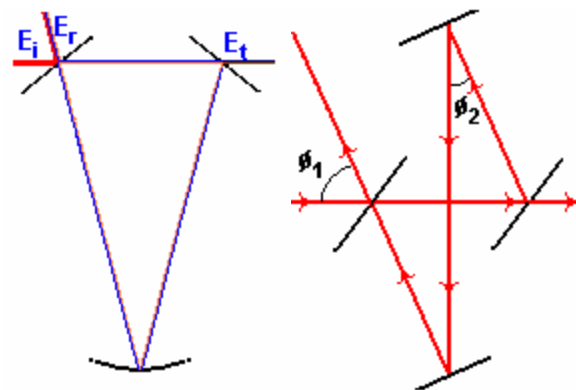


Figure 2a, 2b. (a) 3 Mirror MC (b) 4 Mirror MC.

### 3- v. 4-Mirror Mode Cleaner

The choice of using a 4-Mirror MC, as opposed to a 3-Mirror MC, results from the fact that a laser beam passing through a mode cleaner is not completely symmetric. In terms of ABCD matrices, each non-coupling mirror can be correctly treated in the y dimension as a unity matrix. However, in the x dimension, in the horizontal axis of the laser table, the beam undergoes an inversion with each mirror. If the beam is excited in the x dimension and the cavity has an odd number of flip mirrors, the modes in the x-dimension will experience an overall phase shift of  $\pi$  in one round trip, so they will resonate at a different frequency than the modes in the y-dimension. Therefore, the number of excited modes will effectively be doubled, meaning more noise and more difficult detection. Figure 3 is an illustration of this effect:

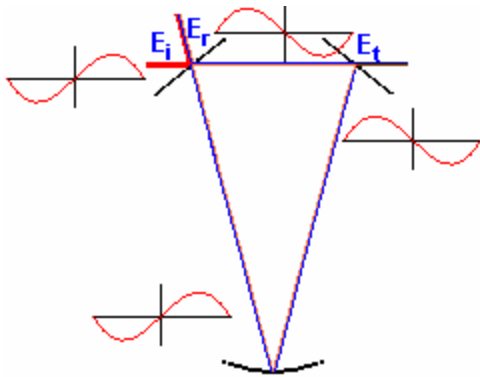


Figure 3. Horizontal inversion of the input signal after one pass through an odd mirror Mode Cleaner configuration.

### Aspect Ratio

The angle  $\theta_1$  (defined in Figure 2b) between the incident and reflected beam determines how much reflected light returns to the IFO, which we want to minimize. However, as the angle  $\theta_1 \rightarrow 90^\circ$ , the inscribed angle,  $\theta_2 \rightarrow 0$ . When  $\theta_2$  is small, some of the light in the cavity will retroreflect, causing counter propagation in the mode cleaner and a build up in the direction opposite the arrows, which will result in extremely high amplitude light leaving the mode cleaner and entering the IFO. The cavity dimensions therefore must be selected such that both angles are significantly larger than 0.

An observant reader might then ask why not select an aspect ratio 1:1,  $\theta_1 = \theta_2$ ? To answer this, there is a further complication: the top mirror is actually a curved mirror, while the other three are flat mirrors. When one of the mirrors is a spherical mirror and the beam comes at an incident angle other than  $0^\circ$ , the beam will have a different waist size in the x and y dimensions.

### Gaussian Beam

As a Gaussian beam propagates, the beam is either converging or diverging. Take a converging beam, and allow it to propagate until the beam has become focused (limited only by diffraction). This point,  $z_0$ , is the beam waist.

For  $z > z_0$ , the beam will begin to diverge. A beam trapped in an optical cavity, but diverging infinitely will quickly vanish. By placing one curved mirror in the cavity, the mirror serves as a focusing lens, such that when the divergent beam reflects off the mirror it is not longer diverging, but converging.

The paraxial beam can be described by a pair of 2-vectors (one for  $x, x'$  and one for  $y, y'$ ). The matrices are used to propagate the beam 2-vector through an optical system. If the optical system is a closed path (such as an optical cavity) that we require to close in on itself (resonance), then the product of the propagation matrices around that path must be the unit matrix. This condition determines the parameters of the (diffraction-limited) resonant beam: the beam waist size and position in x and y.<sup>1</sup>

### G-factor as a Selection Criteria for ROC and Cavity Length

Taking the g-factor discussed in Appendix A.IV, we can plot the HOM transmission against the g-factor, which depends on the cavity length and the ROC. From figure 4 we see that there are regions of the g-factor where small changes in g-factor result in little or no increase in the transmitted HOMs. After selecting a g-factor, a ROC can be selected from the CVI lasers website. The available ROC values are 0.25, 0.3, 0.5, 1, 1.5, 2, 3, 5, 6, 10 m.

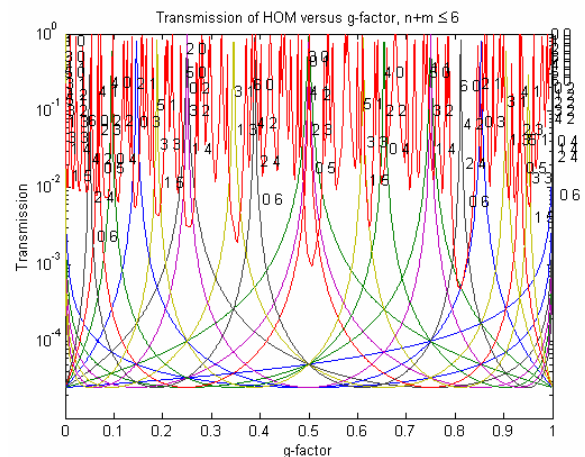


Figure 4. Transmission of the HOM of the mode cleaner with the parameters: ROC 1.000 m (fixed) and aspect ratio held at 1:5.5. Cavity length varied.

From the plot, g-factors ~0.77 and 0.8 produce HOM transmission less than 0.1%. In the end, we decided on L = 0.225 (half-length), for a g-factor of 0.775, as in Fig 5.

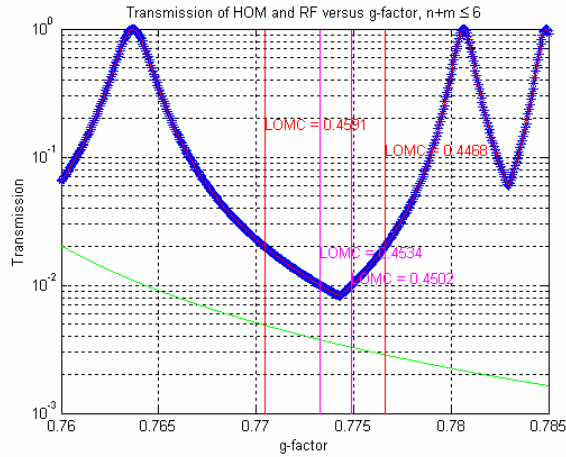


Figure 5. Carrier transmission < 1% for a cavity < 47 cm. RF less than 2% in the range LOMC 44.68-45.91 cm and less than 1% for 45.02 – 45.34 cm

This is the valley we selected because the valley allows more than 2 mm of error in the cavity length, or ~1% error in the ROC (note that CVI mirrors have a ROC tolerance of +0.5%). A drawback to this valley is that the RF transmission, between 1 and 2% for a large portion of the range, is not as low as other areas. Looking at Figure 5, we can see that this g-factor area allows at least 1% margin for error in length and ROC, which is comparable to ROC tolerances for the off-the-shelf mirror that will be used for this OMC.

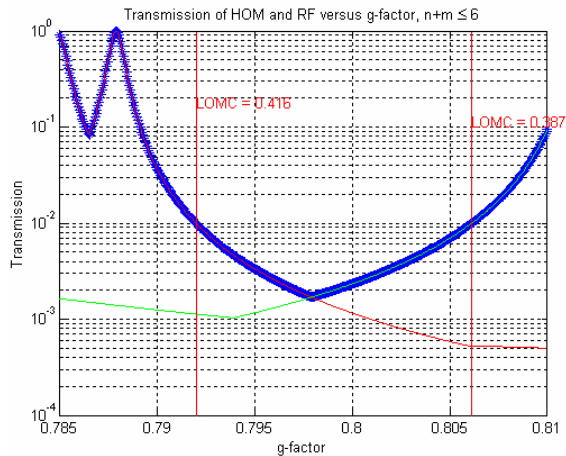


Figure 6. Carrier transmission < 1% for LOMC > 38.78 cm and RF transmission less than 1% for LOMC < 0.416. Total transmission < 1% for LOMC = 0.3878-0.416.

The valley in figure 6 is formed by the intersection of the RF (red line) and the TEM (green line) HOMs. Two very good criteria for selecting this valley are that the valley is very broad and the transmission in the valley is less than 1% for both the carrier and the RF. One drawback is that both the RF and the carrier could appear depending on the amount of carrier and RF present in the input beam.

### Guoy Phase Shift

What can be viewed as the primary purpose for a Mode Cleaner is the ability to allow transmission of only the lowest order resonant mode. A mode cleaner will reflect light at frequencies that differ from the resonant frequency. Higher order Hermite Gaussian modes share the same carrier frequency as TEM<sub>00</sub>, but the mode cleaner can still filter them because of the difference in beam profile. Each mode has a different beam profile, and none is an ideal plane wave. The (the paraxial equation) is<sup>2</sup>:

$$\frac{\partial^2 \psi}{\partial x^2} + \frac{\partial^2 \psi}{\partial y^2} - 2 j k \frac{\partial \psi}{\partial z} = 0$$

The beam has a wavefunction solution

$$u = \psi(x, y, z) e^{-j k z}$$

$$\psi = e^{-j \left( P + \frac{k}{2q} r^2 \right)}$$

Where P is the complex phase shift and q is the complex beam parameter:

$$\frac{1}{q} = \frac{1}{\text{ROC}} - j \frac{\lambda}{\pi \omega^2}$$

, ROC is the radius of curvature of the wavefront, j is the square root of -1, λ is the wavelength, and ω is the waist size

Applying the solution to the wave equations, we get

$$q' = 1$$

$$P' = -\frac{j}{q}$$

At the beam waist, TEM<sub>00</sub> has a planar wavefront, so q<sub>0</sub> = j P<sub>0</sub> ω<sub>0</sub><sup>2</sup> / λ

Solving these differentials, we have

$$q = q_0 + z = j \frac{\pi \omega_0^2}{\lambda} + z$$

$$P' = -\frac{j}{q} = -\frac{j}{z + j \left( \frac{\pi \omega_0^2}{\lambda} \right)}$$

$$j P = \ln \left[ \sqrt{1 + \left( \frac{\lambda z}{\pi \omega_0^2} \right)^2} \right] - j \arctan \left( \frac{\lambda z}{\pi \omega_0^2} \right)$$

q<sub>0</sub> is the complex beam parameter at the beam waist and ω<sub>0</sub> is the beam waist.

Combining these equations, and noting:

$$\sqrt{1 + (\lambda z / \pi \omega_0^2)^2} \approx \frac{\omega_0}{\omega}$$

We have a solution

$$u = \frac{\omega_0}{\omega} e^{-j(kz - \Phi) - r^2 \left( \frac{1}{\omega^2} + \frac{j}{2R} \right)}$$

We see that a propagating paraxial beam picks up an effective phase shift, known as the Guoy phase

$$\Phi = \arctan \left( \frac{\lambda z}{\pi \omega_0^2} \right)$$

In normal operation, the TEM00 mode is made to resonate in the output mode cleaner. The higher order modes will differ in Guoy phase from the TEM00 mode, and will not, in general, resonate; instead, it will be reflected. However, the HOM will be transmitted if the Guoy phase is small enough to fit in the bandwidth of the cavity, or accidentally lands at a multiple of the free spectral range  $f_{FSR} = c/(2L)$  of the cavity. The cavity is designed to avoid this situation for the lowest order HOMs. Figure 7 shows the Guoy phase plotted against the ROC. A more significant quantity to plot against is the g factor, but plotting against the ROC allows selection of a good value to fix the ROC against prior to plotting HOM transmission against g-factor.

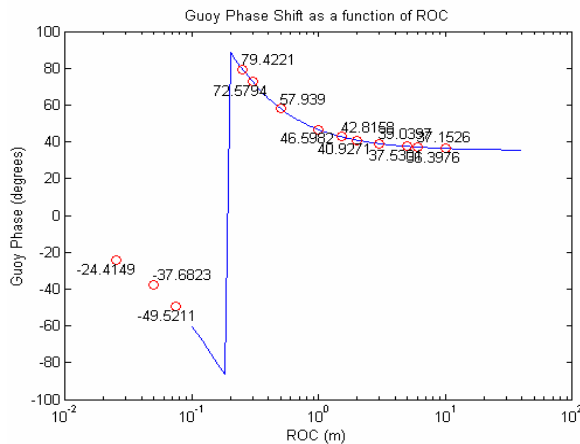


Figure 7. Guoy Phase (or phase shift) as a function of ROC

### Gaussian Beam Waist

One method to find  $x^2$  and  $y^2$ , the square of the beam waists, is to employ the technique of ABCD matrices. Propagation of a beam through an optical system can be expressed in terms of a matrix  $\begin{bmatrix} A & B \\ C & D \end{bmatrix}$ . Elements A and D are dimensionless quantities, while B has dimensions of length and C of inverse length units. The matrix representing propagation through a free space propagator of optical length d is:

$$\begin{pmatrix} 1 & d \\ 0 & 1 \end{pmatrix}$$

d is the optical distance (physical distance divided by index of refraction n, n = 1 in vacuum)

Flat mirrors only fold the beam, and have ABCD matrices that are unity. Curved mirrors have a more complicated ABCD matrix. For an incident angle of 0, and for the case where the radius of curvature is extremely large, they approximate flat mirrors to a high degree, but for significant angle of incidence and ROC the optical cavity ABCD matrix must be resolved as two separate matrices for x and y respectively. The spherical mirror ABCD matrix is:<sup>1</sup>

$$\begin{pmatrix} 1 & 0 \\ -2/R & 1 \end{pmatrix}, \text{ with}$$

$$R = \text{ROC} / \cos \left( \frac{\phi_2}{2} \right) \text{ for } [ABCD]_x \text{ and}$$

$$R = \text{ROC} * \cos \left( \frac{\phi_2}{2} \right) \text{ for } [ABCD]_y.$$

The equation for propagation through an optical medium represented by an [ABCD] Matrix is:

$$q_2 = \frac{Aq_1 + B}{Cq_1 + D}$$

For a beam resonating in a cavity, the input and output complex beam parameters  $q_1 = q_2 = q$ . Using the above relation and the definition for q:

$$\frac{1}{q} = \frac{1}{\text{ROC}} - j \frac{\lambda}{\pi \omega^2}$$

We find that the beam waist is given by the equation:<sup>2</sup>

$$\omega^2 = (2\lambda B / \pi) \sqrt{4 - (A + D)^2}$$

Because  $\lambda/2$  does not equal to zero, one term of the ABCD matrix will differ between the x and y solutions, so the beam waists in x and y do not match. The mismatch in resultant beam waists, calculated as indicated in Appendix A.III, is called astigmatism. For the goal of retaining as much of the input light as possible and at the same time filtering out the higher order modes and RF sidebands, it is beneficial to minimize the astigmatism, which is accomplished by choosing an aspect ratio that minimizes  $\lambda/2$ . In the end, we realized that this consideration was not very important. The issues that mattered were driven by the fact that the reflectivity and transmissivity of the mirrors depend on the incident angle. The input coupler incident angles should be equal, so that their transmissivities are equal (critical coupling); and CVI Laser expects them to be spec'ed at 45 degrees, so we want to be as close as possible to that. The internal mirrors should be as close to 100% reflectivity as possible, so the incident angles should be as close to 0 as possible, since OTS mirrors are made for 0 and 45 degree incidence angles.

We select an aspect ratio with this in mind and plot  $x^2$  and  $y^2$  against ROC (see figure 8) to find a good off-the-shelf ROC.

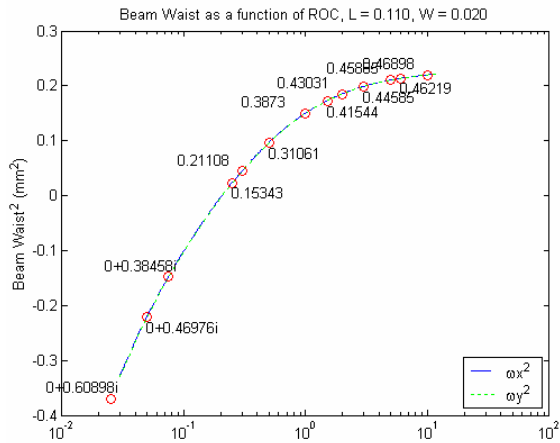


Figure 8. Beam Waist as a Function of ROC

### Transmission of Higher Order Light

The Output Mode Cleaner will allow limited transmission of both RF sidebands and higher order TEMs. The RF sidebands on the carrier beam at the 40m IFO are at frequencies 33.206 and 166.03 MHz. The transmission of the 33 MHz sideband is higher, as it lies closer in to the resonant peak, as seen in Figure 9. The RF TEM<sub>00</sub> transmission has no dependence on the ROC of the spherical mirror, only frequency dependence and dependence on cavity length (the smaller the FSR is, the closer in the RF sidebands to the resonance peak, so the greater transmission for a given linewidth.)

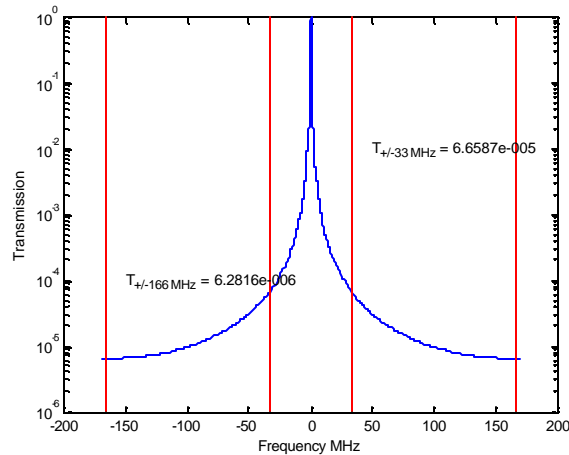


Figure 9. Resonant peak with 33 and 166 MHz RF sideband transmission.

Also, cavity transmission of the higher order TEMs and the RF sidebands is plotted against mirror transmissivity in figure 10. TEM<sub>00</sub> is transmitted at 100%, and the plot is on a logarithmic scale, so the fall off in transmission is very great for low mirror transmissivity. As one would expect, lowering the transmissivity results in decreased transmission of non-resonant light. A plot of this, as well as the transmission at resonance is in figure 10.

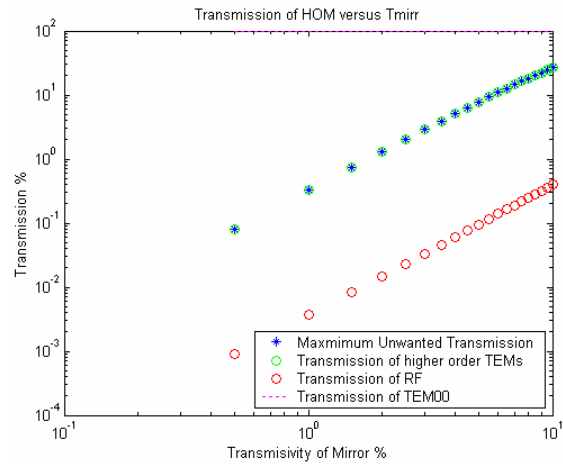


Figure 10. Transmission versus Transmissivity of the mirror

For ROC values < 0.250 m at the initial cavity length the cavity parameters become negative or imaginary. The total cavity length is 0.450 m, and treating the cavity as a half symmetric cavity, the effective cavity length is half that. Then, as is discussed in Appendix A.IV, the g-factor must lie between 0 <math>g < 1</math>, applying the formula for  $g = 1 - \text{LOMC}/\text{ROC}$ . For a stable cavity we must have ROC > 0.225 m. Then an acceptable ROC for a round trip cavity length of ~0.5 m is 1.000 m, giving a g-factor of ~ 0.5. The round trip cavity length we selected for the g-factor we selected and ROC 1.000m is close to this value so ROC 1.000m is a suitable mirror ROC.

## Thermal Expansion and PZT Dynamic Range

The OMC will be constructed from a block of some material that we select, which will serve as a fixed spacer. Changes in temperature cause materials to expand based on the coefficient of thermal expansion for the material. For the OMC, the materials under consideration are glass, aluminum, steel, and invar. Glass (borosilicate) has a thermal expansion coefficient of  $4.78 \times 10^{-6} / \text{K}$  at 293 K from the NIST website<sup>3</sup>. Invar, aluminum, and steel are compared on the Watch and clock magazine website<sup>4</sup>, with Invar having a coefficient of thermal expansion = 0.8-2 ppm / K, steel ~ 11 ppm / K, and aluminum ~ 25.5 ppm / K.

$$\alpha = \frac{\Delta L}{L} \frac{1}{\Delta T}$$

The coefficient of thermal expansion for small changes in temperature the corresponding change in length will be  $\Delta L = \Delta T L \alpha$ . For cavity length 22.5 cm and change in temperature of 1 K, the resulting change in length varies significantly with the material. It is expected that the actual temperature fluctuations will be less than 1 K, and an appropriate expansion in length is no more than a few microns.

Material	Coeff. Therm. Expan. ( $10^6/\text{K}$ )	Expansion ( $\mu\text{m}$ ) for 1K
Aluminum	25.5	5.35
Stainless Steel	11	2.31
Glass	4.78	1.0038
Invar	1.3	0.273
Super Invar	0.63	0.1323

Figure 1. Coefficients of Thermal Expansion and corresponding expansion for temperature variation of 1 K.

While aluminum is the easiest to machine, it also has the largest length change per change in temperature. Super invar has the smallest coefficient of thermal expansion, but is the most difficult to machine and is the most expensive. Glass and invar are relatively expensive, relatively difficult to machine, and have longer delivery lead-times. The numbers for Aluminum and stainless steel, the two with the largest response to temperature appear to be within the acceptable region, while invar is extremely expensive and not as critical.

To lock the laser beam resonance in the cavity, we actuate on the cavity length by moving a mirror attached to a PZT stack. Typical PZT stacks used in this application have a dynamic range of a few microns. The final decision is to use stainless steel, because it is comparable in difficulty of machining and cost to aluminum.

## Mode Matching into the OMC

Having selected the top level cavity parameters (length, number of mirrors, ROC of the curved mirror, and transmissivity of the input and output coupling mirrors), the next concern to consider is to match the input beam mode to the OMC eigenmode. Mode mismatch results in the input beam coupling into the HOMs of the OMC, which is junk light and is not transmitted. Mode mismatch in power (reduction in transmitted power) is the geometric square of the amplitude coupling due to mismatch in beam waist size and locations.

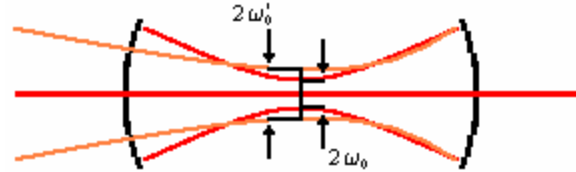


Figure 12. Beam Waist size mismatch, the incident beam has a waist  $\omega_0'$  and the cavity has waist  $\omega_0$ .

To find the mode mismatch here, consider the polar form of the generalized cavity eigenfunctions:<sup>5</sup>

$$V_0(r) = \sqrt{\frac{2}{\pi}} \frac{1}{\omega_0} \exp\left(\frac{-r^2}{\omega_0^2}\right)$$

$$V_1(r) = \sqrt{\frac{2}{\pi}} \frac{1}{\omega_0} \left(1 - \frac{2r^2}{\omega_0^2}\right) \exp\left(\frac{-r^2}{\omega_0^2}\right)$$

If we assume the beam is mostly aligned except that the input beam has a waist size  $\omega_0' = \omega_0(1 + \epsilon)$  where  $\epsilon$  is a small fraction, then the wavefunction for the system is<sup>5</sup>

$$\Psi(r) = A \sqrt{\frac{2}{\pi}} \frac{1}{\omega_0} (1 + \epsilon) \exp\left(\frac{-r^2}{\omega_0^2} (1 + \epsilon)^2\right)$$

expanding in  $\epsilon$  to first order, this gives

$$\Psi(r) = A (V_0(r) + \epsilon V_1(r))$$

The coupling to higher order modes is linear in the fractional deviation of the input beam waist size from the OMC eigenmode waist size. Because this is the beam wavefunction, we square this to get the power mismatch due to beam waist size differences.

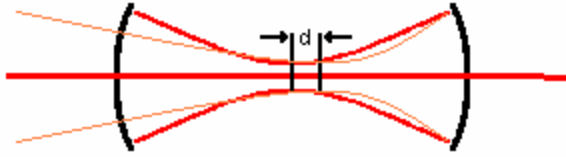


Figure 13 Beam Waist location mismatch, the focal point of the incident beam is a distance d away from the cavity waist.

The other form of mode mismatch occurs when the position of the input beam waist is not correctly matched with the cavity waist. Applying a more generalized form of the polar eigenfunctions with beam width at distance z, where z is measured relative to the beam waist z = 0:

$$V_0(r, z) = \sqrt{\frac{2}{\pi}} \frac{1}{\omega(z)} \exp\left(-r^2 \left( \frac{1}{\omega(z)^2} + j \frac{\pi}{\lambda R(z)} \right)\right)$$

$$V_1(r) = \sqrt{\frac{2}{\pi}} \frac{1}{\omega(z)} \left(1 - \frac{2r^2}{\omega(z)^2}\right) \exp\left(-r^2 \left( \frac{1}{\omega(z)^2} + j \frac{\pi}{\lambda R(z)} \right)\right)$$

$$R(z) = z \left(1 + \left(\pi \frac{\omega_0^2}{\lambda z}\right)^2\right)$$

Axially translating the beam waist input beam to the cavity waist for a small displacement d, input beam radius of curvature and beam waist are:

$$R(d) \sim -d \left( \frac{\pi \omega_0^2}{\lambda d} \right)^2$$

$$\omega^2(d) \sim \omega_0^2$$

such that the wavefunction is then:

$$\Psi(r, d) = \sqrt{\frac{2}{\pi}} \frac{1}{\omega(d)} \exp\left(-r^2 \left( \frac{1}{\omega_0^2} + j \frac{\pi}{\lambda} \left( \frac{1}{-d} \left( \frac{\lambda d}{\pi \omega_0^2} \right)^2 \right)\right)\right)$$

$$\Psi(r, d) = \sqrt{\frac{2}{\pi}} \frac{1}{\omega(d)} \exp\left(\frac{-r^2}{\omega_0^2} \left(1 - j \frac{\lambda d}{\pi \omega_0^2}\right)\right)$$

$$\Psi(r, d) = \sqrt{\frac{2}{\pi}} \frac{1}{\omega(d)} \exp\left(\frac{-r^2}{\omega_0^2} (1 - j\xi)\right)$$

Expanding the exponential term in to first order, the resulting wave function again is:

$$\Psi(r, z) = A (V_0 + (j/2) \xi V_1)$$

$$\Psi(r, z) = A \left( V_0 + j \frac{\lambda d}{2\pi \omega_0^2} V_1 \right)$$

Once again, mode mismatch couples to the first excited state, but this time, with an imaginary coupling (corresponding to a relative phase shift of pi/2).

Summing the two forms of mode mismatch gives a total mode mismatching of:

$$MM^2 = \left( \frac{\omega_0'}{\omega_0} - 1 \right)^2 + \left( \frac{\lambda d}{2\pi \omega_0^2} \right)^2$$

## Output Mode Matching Telescope

To minimize the mode mismatch, we design an OMMT, a series of mirrors including two curved mirrors that focus the input beam as closely as possible to match the OMC beam waist size and position (see figure). The OMMT is designed to make the output beam, which has a mode structure determined by the IFO, match the mode structure of the OMC. Selecting an off the shelf mirror of  $ROC_1 = 618.4$  mm, and then selecting a second mirror to minimize the MM, we find that  $ROC_2 = 150$  mm works well.

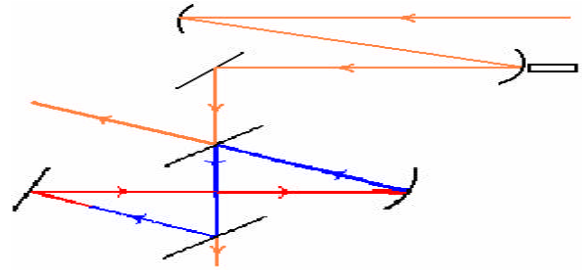


Figure 13. Output Mode Matching Telescope and OMC

The first curved mirror is fixed, but the second curved mirror is on an adjustable mount so that the defocus ( $ROC_1 + ROC_2 + \text{defocus}$  gives the distance separating the two curved mirrors) can be varied. Mike Smith selected the ROC and I verified his choice of ROC, the selected ROC are 618.4 mm for OMMT mirror 1 and 150mm for OMMT mirror 2. The varying the defocus is equivalent to varying the length of the telescope. We can then plot the Mode Mismatch in power against the defocus to find the optimum setup. The mode mismatch should be highly sensitive to the defocus, and the mirror will be adjustable by approximately 1 cm.

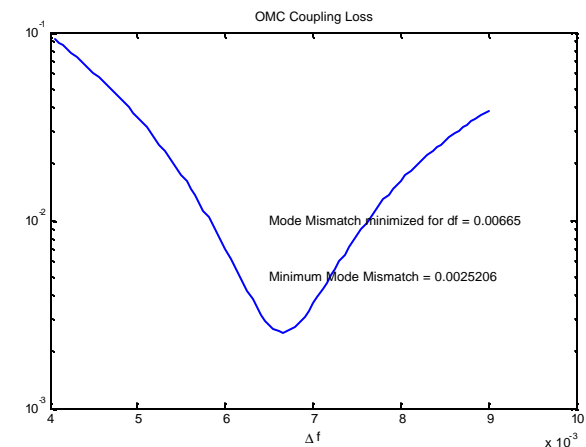


Figure 14. OMC transmitted power loss plotted against the Defocus

From this plot, the most suitable defocus is then 6.7 mm, which produces a power loss of less than 0.25%.

## Conclusion

The mode cleaner to be constructed will have transmission and reflection as shown in Figure 15, which also includes most of the relevant beam parameters. The narrow beam waist and the large Guoy phase will allow filtering of the higher order modes while permitting a high transmission of the desired carrier TEM00 mode light.

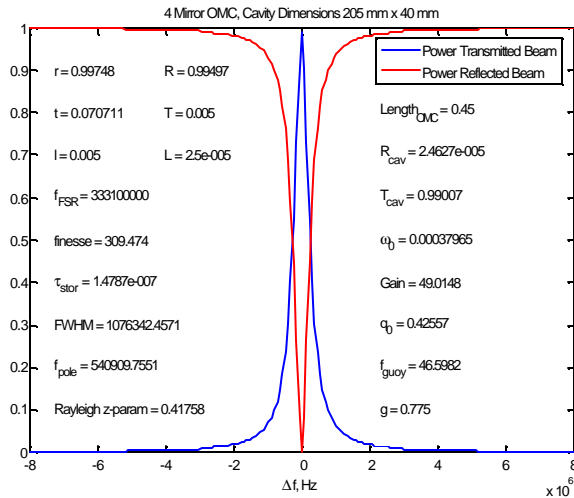


Figure 15. 4 Mirror Output Mode Cleaner Reflection and Transmission plotted against frequency. Cavity specifications included on plot. See Appendix C for definitions of these quantities.

## Construction of the Mode Cleaner and Future Work

The OMC will be constructed from a block of Stainless Steel, with dimensions  $\sim 20.5$  cm by 4 cm. The beam paths will be bored out and the mirrors placed and secured with three mechanical clasps each, except for the PZT mounted mirror, which will be glued onto the PZT with vacuum compatible glue.

Commissioning the output mode cleaner will require setting up the optical cavity, positioning it correctly, aligning the mirrors, creating a control system, and calibrating and fine tuning this control system. Locking of the OMC will be accomplished through a dither locking system.

Another option for locking is to use the Pound-Drever-Hall method, which is used for locking the main interferometer, but is much less desirable for the OMC as a dither-locking system is simpler to construct and implement, and provides a more robust lock. The PDH signal is available only when the cavity is very close to resonance, while the dither signal is always available. For suspended mass cavities, the cavity will swing through resonance often. But for a “fixed spacer” cavity like our OMC, we have to drive it towards resonance with something like a dither-lock system.

Once the mirrors have been selected and the servo system for locking the OMC completely figured out, it will be time to construct and align the OMC.

Once the parts have arrived, it will be possible to set up the cavity and experimentally observe the behavior of the output beam that passes through the output mode cleaner. The mirrors will be ordered as soon as possible, and will hopefully arrive with reasonable time to complete the project. The interferometer setup already exists, as does the software for control of the laser system. This will be an addition to LIGO 40m setup.

## References

1. Siegman, Anthony. Lasers. University Science Books: Sausalito. 1986.
  2. Kogelnik, H. and T. Li. "Laser Beams and Resonators," Proceedings of the IEEE., vol. 54, no. 10, pp. 1312-1329. October 1966.
  3. "NIST SRM Order Request System", Certificate of Analysis Borosilicate. [https://srmors.nist.gov/certificates/view\\_cert2gif.cfm?certificate=731](https://srmors.nist.gov/certificates/view_cert2gif.cfm?certificate=731), NIST, 12 September 2005.
  4. "Watch and clock magazine – Invar in horology". <http://www.orologeria.com/english/magazine/magazine3.htm>, 12 September 2005.
  5. Anderson, Dana Z. "Alignment of resonant Optical Cavities," Applied Optics., vol. 23, no. 17, pp. 2944-2949. September 1984.
- Black, Eric. Physics 77. Caltech Senior Physics Atomic Laboratory Class.
- Libbrecht, Kenneth. Physics 76. Caltech Senior Physics Laser Laboratory Class.
- Smith, Micheal. Mini Lecture and discussion on Mode Matching and Output Mode Matching Telescope.
- Ward, Robert. Mini Lectures and discussions on Fabry-Perot cavities, Mode Cleaners, Pound-Drever-Hall and dither-locking.
- Weinstein, Alan J. Mini Lectures and talks on various aspects of LIGO.
- Yariv, Amnon. Introduction to Optical Electronics. Holt, Rinehart and Winston: New York 1976.

## Appendix A: The Physics Behind a Fabry-Perot Cavity

A Fabry-Perot Cavity can take on a number of forms with a number of mirrors. However, the two significant mirrors are the input and output coupling mirrors. All other intermediate mirrors and lenses serve only to fold the beam and contribute to the cavity loss.

### I. A Simple Fabry-Perot Cavity

For this discussion, let us take two non-ideal input and output couplers with optical coefficients  $r_i$ ,  $t_i$ ,  $l_i$ ,  $r_o$ ,  $t_o$ ,  $l_o$  respectively for amplitude reflectivity, transmissivity, and losses due to scattering and absorption for the input and output couplers.

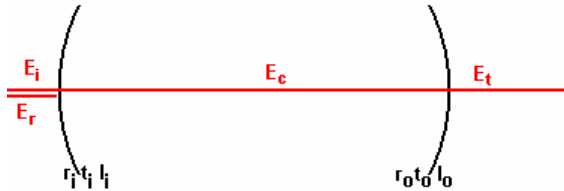


Figure A-1. Simple Fabry-Perot cavity

The power reflectivity, transmissivity, and loss go as the modulus squared of the respective amplitude coefficients:

$$\begin{aligned} R_I &= |r_I|^2 && \text{power reflectivity} \\ T_I &= |t_I|^2 && \text{power transmissivity} \\ L_I &= |l_I|^2 && \text{power loss} \\ R_I + T_I + L_I &= 1 && \text{conservation of energy} \end{aligned}$$

It is a simple exercise to calculate the electric field in each of the three regions: circulated, reflected, and transmitted.

$$\begin{aligned} E_c &= E_i t_I + E_c r_I e^{ikL} r_o e^{ikL} \\ &= E_i t_I + E_c r_I r_o e^{i2kL} \\ E_c &= E_i \frac{t_I}{1 - r_I r_o e^{i2kL}} \\ &= E_i \frac{t_I}{1 - r_I r_o e^{i2\phi}} \end{aligned}$$

The reflected beam can be calculated in a similar manner, as it has a contribution from the promptly reflected light, as well as an infinite number of contributions (neglecting loss due to power) from the beam circulating in the cavity, as pictured in figure A-2. Each successive reflection of the beam picks up an  $r_I r_o e^{i2\phi}$ . Summing the terms to infinity, we have:

$$E_r = -E_i r_I + E_i t_I / r_I \sum_{n=0}^{\infty} (r_I r_o e^{i2\phi})^n$$

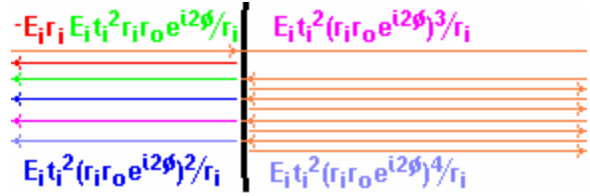


Figure A-2. Reflected Beams, the Prompt Reflection is in Red, the first four terms in the sum due to the circulating beam are displayed in Green, Magenta, Blue, and Violet.

$$\begin{aligned} E_r &= \frac{E_i}{r_I} \left( T_I \sum_{n=1}^{\infty} (r_I r_o e^{i2\phi})^n - R_I \right) \\ &= \frac{E_i}{r_I} \left( T_I \frac{r_I r_o e^{i2\phi}}{1 - r_I r_o e^{i2\phi}} - R_I \right) \\ &= \frac{E_i}{r_I} \frac{T_I r_I r_o e^{i2\phi} - R_I + R_I r_I r_o e^{i2\phi}}{1 - r_I r_o e^{i2\phi}} \\ E_r &= E_i \frac{(1 - L_I) r_o e^{i2\phi} - r_I}{1 - r_I r_o e^{i2\phi}} \end{aligned}$$

This result is identical to the one obtained by considering the reflected beam to simply be the circulating beam reflected off output mirror  $r_o$ , propagated twice the cavity length picking up a phase  $e^{i2\phi}$ , and then transmitted through the input mirror  $t_i$  with the promptly reflected beam added in.

A similar argument can be employed to find the transmitted amplitude. The first term in the sum representing the transmitted amplitude is simply  $E_i t_i t_o e^i$ , and each additional term picks up  $r_I r_o e^{i2\phi}$ . Or considering the transmitted beam in terms of the circulating beam, propagate  $E_c$  through one cavity length, or a phase of  $e^i$ , then through the output coupler  $t_o$ .

$$\begin{aligned} E_t &= E_i t_I t_o e^{i\phi} \sum_{n=0}^{\infty} (r_I r_o e^{i2\phi})^n \\ E_t &= E_i \frac{t_I t_o e^{i\phi}}{1 - r_I r_o e^{i2\phi}} \end{aligned}$$

Measuring  $E_i$  in units of  $\sqrt{P}$ , the power reflected and transmitted are just the square of the reflected and transmitted amplitudes, as in figure A-3. The reflected power is very close to unity everywhere except in the region surrounding cavity resonance, where the reflected power approaches zero, while the transmission is close to 0 everywhere except close to resonance, when transmitted power approaches unity (for an ideal cavity).

$$\begin{aligned} P_r &= |E_r|^2 \\ P_t &= |E_t|^2 \end{aligned}$$

## II. Resonance Condition and Characteristics

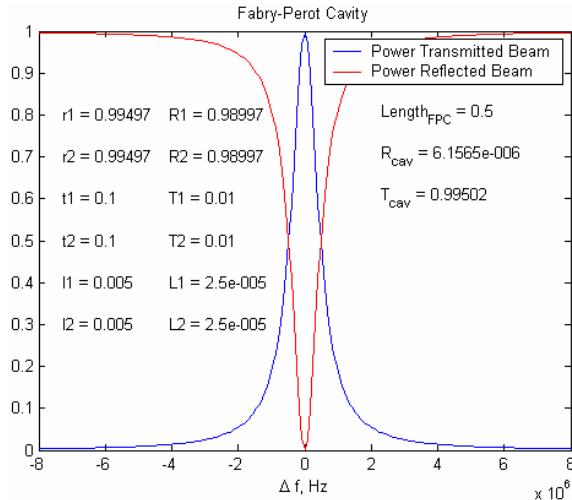


Figure A-3. Transmission and Reflection for a typical Fabry-Perot cavity.

The defining characteristic of a Fabry-Perot cavity is the extreme sensitivity to the desired resonance, while rejecting other frequencies.

Consider the above equations; resonance occurs when the denominator term is minimized, which occurs when the phase term goes to unity, or  $2\phi = 2\pi n$  for integer values of  $n$ . Then a Fabry-Perot cavity has resonance for  $\phi = \pi n$ , or:

$$\begin{aligned}\phi &= kL = \frac{2\pi}{\lambda} L \\ &= 2\pi \frac{L}{\lambda} = 2\pi f \frac{L}{c} \\ &= \pi n \\ f &= \frac{c}{2L} n \quad L = n \frac{\lambda}{2} \\ f_{\text{FSR}} &= \frac{c}{2L}\end{aligned}$$

Where  $f_{\text{FSR}}$ , the free spectral range, is the frequency spacing between resonant peaks, and the cavity has resonance when the cavity length is equal to an integral number of half wavelengths.

Transmission is close to unity at resonance, and off resonance it falls off to zero very quickly. For different cavity parameters, the frequency range before the transmission falls off significantly can vary greatly. The steepness of the resonance curve, which determines the frequency response, is called the finesse. Measuring the bandwidth of the peak as the full width at half maximum, the finesse is defined simply as the distance between cavity peaks divided by the cavity width. The FWHM or bandwidth can be calculated from the point where the resonance peak has fallen off by  $1/2$  for power, or  $1/\sqrt{2}$  for field

amplitude. Since the dominant resonance term is due to the  $1 - r_1 r_0 e^{i2\phi}$ , we need only find when this term squared doubles the squared resonance denominator.

Using delta notation, where  $\delta_c$  is the cavity loss term, we can then solve for the finesse, and bandwidth in terms of the  $f_{\text{FSR}}$ ,

$$\begin{aligned}\Delta\omega_{\text{cav}} &= \frac{2\pi c}{2L} \left( \frac{\delta_c}{\pi \sqrt{1 - \delta_c}} \right) = 2\pi f_{\text{FSR}} \left( \frac{\delta_c}{\pi \sqrt{1 - \delta_c}} \right) \\ &= \Delta\omega_{\text{FSR}} \left( \frac{\delta_c}{\pi \sqrt{1 - \delta_c}} \right) \\ \text{finesse} &= \frac{\pi \sqrt{1 - \delta_c}}{\delta_c}\end{aligned}$$

## III. Beam Waist: Locating and Quantifying

The beam waist is the smallest beam diameter along the beam trapped in the cavity (cavity eigenmode). Locating the beam waist is an exercise in geometry: for a 2-curved mirror cavity, locating the beam waist depends on the two radii of curvatures. For a four-mirror mode cleaner, there is only one curved mirror, but a resonating beam will see the same curved mirror twice along its path, at the start and end, so it is equivalent to a two-mirror cavity where both mirrors have identical radii of curvature.

When both mirrors have the same radii of curvature, it is clear through a simple symmetry argument that the beam waist is located halfway between the two mirrors. For a cavity of length  $L$ , the beam waist is located a distance  $L/2$  from the input coupler, and for a mode cleaner with length  $L$ , the beam waist is located at a distance  $L/2$  along the beam path from the curved mirror, see figure A4.

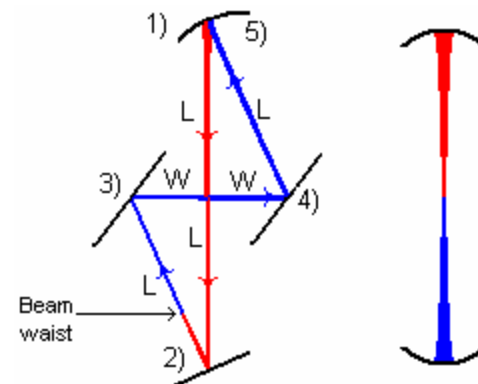


Figure A4. 1) Beam converging 2) converging beam reflected, still converging until it reaches the beam waist, at which point the beam begins diverging 3) Divergent beam reflects off mirror 4) Divergent beam reflects off mirror 5) divergent beam reflects off curved mirror, becoming convergent once again.

The size of the beam, or beam waist, can be calculated by representing the cavity with the ABCD ray matrices. As discussed above, the relevant ABCD matrices are

$$\begin{pmatrix} 1 & 3L \\ 0 & 1 \end{pmatrix} \begin{pmatrix} 1 & 0 \\ -\frac{2L}{R\sqrt{L^2+\frac{W^2}{4}}} & 1 \end{pmatrix} \begin{pmatrix} 1 & L+2W \\ 0 & 1 \end{pmatrix} =$$

$$\begin{pmatrix} 1 - \frac{12L^2}{R\sqrt{4L^2+W^2}} & 4L+2W - \frac{12L^2(L+2W)}{R\sqrt{4L^2+W^2}} \\ -\frac{4L}{R\sqrt{4L^2+W^2}} & 1 - \frac{4L(L+2W)}{R\sqrt{4L^2+W^2}} \end{pmatrix}$$

[A B;C D]<sub>x</sub>

and

$$\begin{pmatrix} 1 & 3L \\ 0 & 1 \end{pmatrix} \begin{pmatrix} 1 & 0 \\ -\frac{\sqrt{4L^2+W^2}}{LR} & 1 \end{pmatrix} \begin{pmatrix} 1 & L+2W \\ 0 & 1 \end{pmatrix} =$$

$$\begin{pmatrix} 1 - \frac{12L^2}{R\sqrt{4L^2+W^2}} & 4L+2W - \frac{12L^2(L+2W)}{R\sqrt{4L^2+W^2}} \\ -\frac{4L}{R\sqrt{4L^2+W^2}} & 1 - \frac{4L(L+2W)}{R\sqrt{4L^2+W^2}} \end{pmatrix}$$

[A B;C D]<sub>y</sub>

Now applying the ABCD law,

$$q_2 = \frac{A q_1 + B}{C q_1 + D}$$

and requiring self consistency (the beam parameter must be the same even after multiple resonant passes through the cavity)

$$q_1 = q_2 = q$$

results in the quadratic solution:

$$\frac{1}{q} = \frac{D-A}{2B} \mp \frac{j}{2B} \sqrt{4 - (A+D)^2}$$

taking the imaginary portion and equating this with the complex beam parameter

$$\frac{1}{q} = \frac{1}{R} - j \frac{\lambda}{\pi \omega^2}$$

solving for  $\omega^2$ , the squared beam waist,

$$\omega^2 = \frac{2B\lambda}{\pi \sqrt{4 - (A+D)^2}}$$

Thus there is a limiting condition, when  $4 - (A+D)^2 < 0$ , the beam waist becomes imaginary, so we want to select parameters to avoid that.

A plot of the cavity waists  $\omega_x^2$  and  $\omega_y^2$  by varying cavity length with the cavity width fixed, thus effectively plotting the waist against the aspect ratio, for a fixed ROC = 300 mm, allows selection of the cavity dimensions, see figure A5.

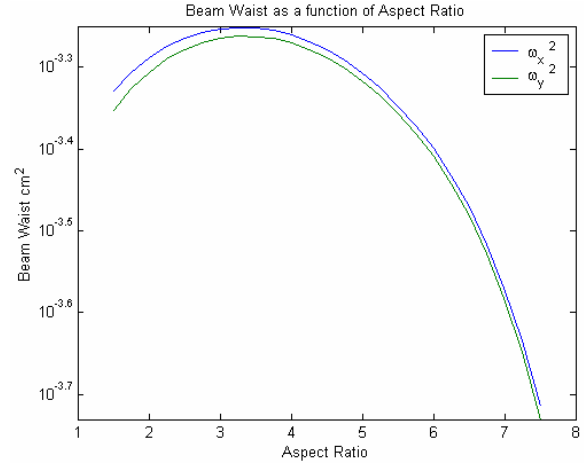


Figure A5. Beam Waist versus Aspect Ratio

#### IV. Cavity Stability: The g-factor

An important quantity in understanding an optical cavity is the cavity g-factor. The g-factor is calculated as:

$$g_1 = 1 - \frac{L}{R_1} \quad \text{and} \quad g_2 = 1 - \frac{L}{R_2}$$

these parameters can be used to express the beam parameters  $z_R$ ,  $z_1$ , and  $z_2$ , the Rayleigh range, and the location of the two end mirrors relative to the beam waist.

$$z_R^2 = \frac{g_1 g_2 (1 - g_1 g_2)}{(g_1 + g_2 - 2 g_1 g_2)^2} L^2$$

$$z_1 = \frac{g_2 (1 - g_1)}{g_1 + g_2 - 2 g_1 g_2} L$$

$$z_2 = \frac{g_1 (1 - g_2)}{g_1 + g_2 - 2 g_1 g_2} L$$

The beam waist can also be expressed in terms of the g-parameter, as well as the spot size at the mirrors

$$\omega_0^2 = \frac{L\lambda}{\pi} \sqrt{\frac{g_1 g_2 (1 - g_1 g_2)}{(g_1 + g_2 - 2 g_1 g_2)^2}}$$

$$\omega_1^2 = \frac{L\lambda}{\pi} \sqrt{\frac{g_2}{g_1 (1 - g_1 g_2)}}$$

$$\omega_2^2 = \frac{L\lambda}{\pi} \sqrt{\frac{g_1}{g_2 (1 - g_1 g_2)}}$$

The g-factor is a measure of cavity stability because only for a particular range of  $R_1$  and  $R_2$  values will the cavity parameters all be real. This stability condition occurs when  $0 < g_1 g_2 < 1$ .

The g-factor is simplified for a symmetric cavity:  $g_1 = g_2 = g$ . Additionally, a symmetric cavity is equivalent to a half symmetric cavity with half the cavity length. If this assumption is made, then  $R_1$  is infinite, so  $g_1 = 0$ , while  $g_2 = g$ . It then becomes more convenient to select the cavity parameters in terms of the g-factor. Once a suitable g-factor has been selected, it is much simpler to pick the available ROC based on the approximate desired cavity length, and the cavity length may be further optimized once the ROC is determined.

### V. Hermite-Gaussian Size

The higher-order mode sizes increase for larger  $n, m$  indices. For a rectangular symmetric cavity, the transverse mode half width scales as  $\sqrt{n} \times \omega$  where  $\omega$  is the principle or ground state  $TEM_{00}$  beam waist and  $n$  has minimum value of 1. This is the  $x$  spatial beam half width, while the  $y$  spatial beam half width is determined as  $\sqrt{m} \times \omega$ . The curved cavity mirror is a one inch curved mirror with clear aperture greater than 85% center diameter, so the effective mirror aperture is 0.0216 m. Because the mirror has a circular aperture, the significant spot size at the plane of the aperture (the mirror) only matters for the maximum beam width. The maximum beam width for  $TEM_{nm}$  is then  $\sqrt{4 n \omega_x^2 + 4 m \omega_y^2} = 2 \sqrt{n \omega_x^2 + m \omega_y^2}$  where  $\omega_x$  and  $\omega_y$  are the  $x$ - and  $y$ -spot sizes on the curved mirror. A plot of the maximum spot size for a Hermite Gaussian beam with indices from  $n = 0$  to  $n = 100$  and  $m = 0$  to  $m = 100$  is in figure A6.

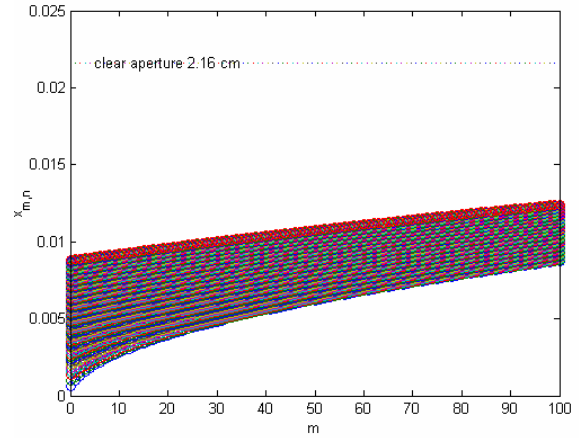


Figure A6. Spot size at curved mirror for  $n, m$  indices each from 0 to 100

Even the  $TEM_{100,100}$  mode, which has the largest spot size, is much smaller than the clear aperture diameter, so this method cannot be used to limit the higher order modes.

## Appendix B: Final Summary of Work

### Week 1:

Finish all administrative/safety details

Understand ABCD Matrices and how to use the eigenvalue Beam Parameters.

### Week 2:

Finish background assignment on making plots and understanding Gaussian Beams

Figure out parameters for input coupling mirror and other mirrors based on how Radius of Curvature and reflectivities affect transmitted beam.

Review the basics, plot and explain in detail Fabry -Perot cavities, the LIGO Michelson IFO, and the 4-mirror OMC.

First Draft of Paper.

### Week 3:

Look at beam width/spot size on the mirrors to determine which HOM will be relevant for filtering and which will be so large that we can ignore their resonance.

Figure out parameters for input coupling mirror and other mirrors based on how g-factor (length and Radius of Curvature) and reflectivities affect transmitted beam.

Look at dither-locking technique for locking the optical cavity.

### Week 4:

Meeting to finalize OMC design. Modify and refine plots to better determine specs for OMC. Decide on material: glass, Al, steel, or invar.

### Week 5:

Finalize the specs for the OMC configuration, as well as the material for construction. Thursday 14, 2005 held a meeting where it was finalized to be a 4-mirror OMC as opposed to a 3-mirror OMC. Also decided on Steel as opposed to Invar, Glass, or Aluminum.

### Week 6:

Update OMC code to match current specs. Model mode matching. Verify calculations made by Mike Smith.

### Week 7:

Second Draft of Paper, and Abstract prepared. Begin coding for error calculations based on transverse displacement, angular misalignment, and mode mismatching of the beam.

### Week 8:

Meet with Mike Smith and discuss Mode Matching. Also find out setup and design of the OMMT and the position relative to the OMC.

### Week 9:

Finish Mode matching code. Hanford Trip.

### Week 10:

Prepare and deliver presentation. Revise paper, prepare for submission.

## Appendix C: Some Vocabulary and Definitions

- r: amplitude reflectivity of an optical system (lens, mirror, FP cavity, ...)
- R: power reflectivity of an optical system (lens, mirror, FP cavity, ...)
- t: amplitude transmissivity of an optical system (lens, mirror, FP cavity, ...)
- T: power transmissivity of an optical system (lens, mirror, FP cavity, ...)
- l: amplitude loss of an optical system (lens, mirror, FP cavity, ...)
- L: power loss of an optical system (lens, mirror, FP cavity, ...)
- $f_{\text{FSR}}$ : free spectral range, the frequency spacing between one resonant peak and the next. It is calculated from the formula  $c/(2 \times \text{half-length})$  (or,  $1/2$  of the round trip path length)
- finesse: Ratio of resonance peak width (FWHM) to peak spacing (FSR),  $\pi \times \sqrt{1 - \text{deltac}} / \text{deltac}$
- $t_{\text{stor}}$ : average time beam spends trapped in the optical cavity before intensity dies off due to loss and transmission.  $\text{fin} / (2 \times \pi \times \text{FSR})$
- FWHM: Full Width at Half Maximum of a resonance peak, usage here is in frequency space with reference to the bandwidth, this is a measure of how wide the cavity is when the transmission is exactly half the transmission at resonance
- $f_{\text{pole}}$ : The cavity pole frequency, inverse of the storage time, it is another measure of the cavity width, but when the cavity transmission has reduced to  $1/e$
- $z_R$ : Rayleigh z-parameter, is the distance the beam travels from the waist before it doubles in area.  $\sqrt{(\text{gfac} / (1 - \text{gfac})) \times \text{LOMC} / 2}$
- $\text{Length}_{\text{OMC}}$ : total optical length (in vacuum) of the mode cleaner, the round trip length of a cavity is typically twice this length.
- $R_{\text{cav}}$ : the total power reflectivity of the cavity
- $T_{\text{cav}}$ : the total power transmissivity of the cavity
- $w_0$ : cavity waist
- Gain: cavity gain,  $T / (1 - R)$
- q: complex beam parameter,  
 $1/q = 1/\text{ROC} - j / (p \times w_0^2)$   
At the beam waist, where the wave front is planar.  $q_0 = j \times w_0^2 / \lambda$
- $\phi_{\text{guoy}}$ : phase shift due to the curvature of the wave front not matching the cavity. In this work, we are employing the fact that the HOM have large Guoy phases, so they will be off resonance.
- HOM: a higher order mode of the transverse extent of a paraxial beam, expanded in Hermite Gaussians
- TEM: Transverse electro-magnetic modes. There are also TE and TM modes (in dielectric media), so TEM modes are to be distinguished from these.
- g: g-factor, this is a measurement of the cavity stability. When  $0 < g < 1$ , the cavity will have real cavity parameters, and will have negligible diffraction losses if the mirrors are big enough